This article was downloaded by: [Institute of Mechanics]
On: 02 September 2014, At: 00:03
Publisher: Taylor & Francis
Informa Ltd Registered in England and Wales Registered Number: 1072954 Registered office: Mortimer House, 37-41 Mortimer Street, London W1T 3JH, UK

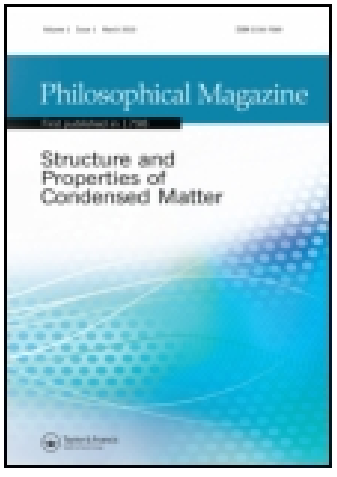

Philosophical Magazine
Publication details, including instructions for authors and subscription information:
http://www.tandfonline.com/loi/tphm20

Dimension limit for thermal shock failure

Y.F. Shao[a], Q.N. Liu[b], H.J. Tian[a], Z.K. Lin[a], X.H. Xu[a] & F. Song[a]
[a] State Key Laboratory of Nonlinear Mechanics (LNM), Institute of Mechanics, Chinese Academy of Sciences, Beijing 100190, China
[b] Aerospace Research Institute of Materials & Processing Technology, Beijing 100076, China
Published online: 18 Jun 2014.

CrossMark
Click for updates

To cite this article: Y.F. Shao, Q.N. Liu, H.J. Tian, Z.K. Lin, X.H. Xu & F. Song (2014) Dimension limit for thermal shock failure, Philosophical Magazine, 94:23, 2647-2655, DOI: 10.1080/14786435.2014.926408

To link to this article: http://dx.doi.org/10.1080/14786435.2014.926408

PLEASE SCROLL DOWN FOR ARTICLE

Taylor & Francis makes every effort to ensure the accuracy of all the information (the "Content") contained in the publications on our platform. However, Taylor & Francis, our agents, and our licensors make no representations or warranties whatsoever as to the accuracy, completeness, or suitability for any purpose of the Content. Any opinions and views expressed in this publication are the opinions and views of the authors, and are not the views of or endorsed by Taylor & Francis. The accuracy of the Content should not be relied upon and should be independently verified with primary sources of information. Taylor and Francis shall not be liable for any losses, actions, claims, proceedings, demands, costs, expenses, damages, and other liabilities whatsoever or howsoever caused arising directly or indirectly in connection with, in relation to or arising out of the use of the Content.

This article may be used for research, teaching, and private study purposes. Any substantial or systematic reproduction, redistribution, reselling, loan, sub-licensing, systematic supply, or distribution in any form to anyone is expressly forbidden. Terms &

Conditions of access and use can be found at http://www.tandfonline.com/page/terms-and-conditions

Downloaded by [Institute of Mechanics] at 00:03 02 September 2014

Philosophical Magazine, 2014
Vol. 94, No. 23, 2647–2655, http://dx.doi.org/10.1080/14786435.2014.926408

Taylor & Francis
Taylor & Francis Group

Dimension limit for thermal shock failure

Y.F. Shao[a], Q.N. Liu[b], H.J. Tian[a], Z.K. Lin[a], X.H. Xu[a] and F. Song[a]*

[a]*State Key Laboratory of Nonlinear Mechanics (LNM), Institute of Mechanics, Chinese Academy of Sciences, Beijing 100190, China;* [b]*Aerospace Research Institute of Materials & Processing Technology, Beijing 100076, China*

(*Received 30 March 2014; accepted 15 May 2014*)

We analytically present the characteristic dimensional limit below which the thermal shock failure of ceramics never occurs. This limit, together with the critical temperature difference, separates the state space of the ceramics under thermal shock into two parts – the cracked and the uncracked. Based on the water-quench tests of ceramics, we experimentally proved that when the states of ceramics are in the uncracked region, the ceramics do not produce any cracks during thermal shock. The results provide a guide to prevent thermal shock failure in ceramic.

Keywords: thermomechanical; ceramics; fracture; thermal shock

Downloaded by [Institute of Mechanics] at 00:03 02 September 2014

1. Introduction

Thermal shock failure of ceramics widely occurs in the thermostructural applications of ceramics. More than one-third of the rejections of ceramic components are caused by thermal shock [1]. Previous studies point out that besides the properties of materials, two external factors of ceramics, the characteristic dimension and the temperature difference, play a key role in the thermal shock failures of ceramics [2–7]. For example, the thermal shock resistance of ceramics increases with the decrease of characteristic dimensions [2–4], and ceramics are prone to thermal shock failures at higher temperature differences [2–4,7]. However, the quantitative effects of the two factors on the thermal shock failures of ceramics have not been understood very well [8]. In this study, firstly, we obtained a relationship between the two critical external factors of ceramics and thermal shock failures based on the theories of heat transfer and thermal stresses. Then, from the water quench tests of alumina, the relationship presented here proved to be in good agreement with the experimental results.

2. Experimental details

The ceramics studied here were alumina balls (purity 99.5%, Xiongdi material Co., Jiyuan, China) with the radius of 0.11, 0.35, 0.56, 1 and 2.1 mm, respectively. The balls were made of Al_2O_3 powder (particle size 0.5 μm, Xiongdi material Co.,

*Corresponding author. Email: songf@lnm.imech.ac.cn

© 2014 Taylor & Francis

Jiyuan, China) and subsequently sintered at 1650 °C for 2 h without pressure. The porosity of ceramics was calculated by measuring its dimension and weight, and the porosity value was about 4.9%.

The balls as-sintered were used in thermal shock. Six specimens in each size group were heated at a rate of 10 °C/min to a preset temperature and were held at this temperature for 20 min. After that the heated specimens were dropped by free fall within five seconds into a water bath which was maintained at 20 °C by a thermostat. After being taken out and dried at 80 °C for 2 h, the specimens were then impregnated with a blue dye (Shanghai ink factory, Shanghai, China) to observe the cracks formed during thermal shock. Afterwards, the crack patterns were studied using stereo microscope (SZ66, Chongqing ott optical instrument Co., Ltd, Chongqing, China).

Downloaded by [Institute of Mechanics] at 00:03 02 September 2014

3. Results and discussion

Thermal shock cracks on the surfaces of the spheres with different radii R at different temperature differences ΔT are shown in Figure 1(a)–(e). As indicated, the cracks occur on the surface of the sphere with $R = 2.1$ mm only when the ΔT between ceramic and water bath is greater than 240 K; and in the case of $R = 0.35$ mm, $\Delta T > 620$ K is needed; however, even if $\Delta T = 1280$ K, the sphere with $R = 0.11$ mm still has no crack. As a result, the occurrence of crack increases with increasing ΔT, but decreases with decreasing R.

Based on experiments, we consider a ceramic sphere of radius R, with a uniform initial temperature T_0. At the initial time, the surface of the sphere is suddenly exposed to a convective medium with a uniform temperature T_∞, as shown in Figure 2.

The temperature field change in the sphere $T = T(r, \tau)$ satisfies the equation of heat conduction

$$\frac{\partial T}{\partial \tau} = \frac{a}{r}\frac{\partial^2}{\partial r^2}(rT), \tag{1}$$

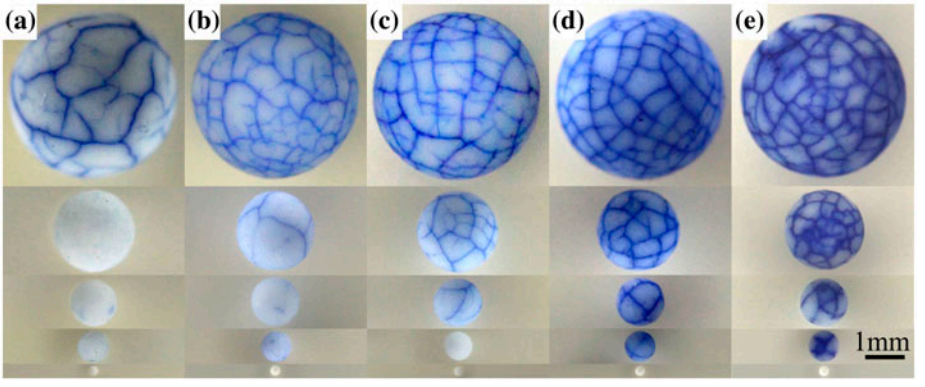

Figure 1. (colour online) Thermal shock cracks on the surfaces of the spheres with different radii, $R = 2.10$, 1.00, 0.56, 0.35 and 0.11 mm (from top to bottom), at the temperature differences ΔT = (a) –280 K; (b) –380 K; (c) –580 K; (d) –780 K; and (e) –1280 K.

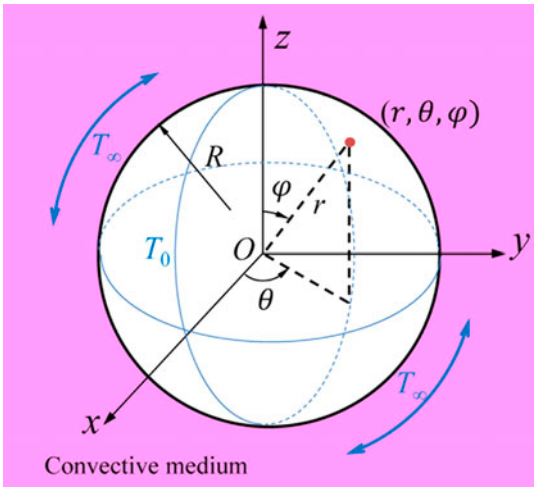

Figure 2. (colour online) A ceramic sphere with radius R and initial temperature T_0 was suddenly exposed to a convective medium of temperature T_∞.

where r is the coordinate, the origin of which is accorded with the centre of the sphere; τ is the time; $a = k/\rho c_p$ is the thermal diffusivity of the material of the sphere; and k, ρ and c_p are the thermal conductivity, the density and the specific heat at constant pressure for the material, respectively.

The initial and boundary conditions that Equation (1) satisfied are written by

$$T(r, 0) = T_0, \tag{2}$$

$$\left.\frac{\partial T}{\partial r}\right|_{r=0} = 0, \tag{3}$$

and

$$-k\left.\frac{\partial T}{\partial r}\right|_{r=R} = h(T - T_\infty), \tag{4}$$

where h is the surface heat transfer coefficient between the sphere and the medium.

Assuming that the properties of the material do not vary with temperature, we can use the standard separation-of-variables technique to solve Equation (1) and obtain the following [9]

$$\frac{T - T_0}{T_\infty - T_0} = 1 - \sum_{n=1}^{\infty} A_n \exp(-\beta_n^2 \cdot f)\frac{\sin(\beta_n \cdot r^*)}{\beta_n \cdot r^*}, \tag{5}$$

where

$$A_n = 2 \cdot \frac{\sin(\beta_n) - \beta_n \cos(\beta_n)}{\beta_n - \sin(\beta_n)\cos(\beta_n)}, \tag{6}$$

Downloaded by [Institute of Mechanics] at 00:03 02 September 2014

and $f = a\tau/R^2$ is Fourier's number that describes the dimensionless time of heat conduction; $r^* = r/R$ stands for the dimensionless coordinate; and β_n are the roots of the equation

$$1 - \beta_n \cot(\beta_n) = \beta, \tag{7}$$

where $\beta = hR/k$ is the Biot number, which is treated as a dimensionless constant in the traditional theories of heat transfer and thermal stresses.

According to the theory of thermal stresses [10], we readily write the thermal stress field in the sphere as

$$\sigma_r(r,\tau) = \frac{2\alpha E}{1-v} \cdot \left[\frac{1}{R^3} \int_0^R (T - T_0) r^2 dr - \frac{1}{r^3} \int_0^r (T - T_0) r^2 dr \right], \tag{8}$$

$$\sigma_\theta(r,\tau) = \sigma_\phi(r,\tau) = \frac{\alpha E}{1-v} \cdot \left[\frac{1}{R^3} \int_0^R (T - T_0) r^2 dr + \frac{2}{r^3} \int_0^r (T - T_0) r^2 dr - (T - T_0) \right], \tag{9}$$

where E, v and α are Young's modulus, Poisson's ratio and coefficient of thermal expansion of the material, respectively.

For the convenience of comparing the values of thermal stresses, the dimensionless thermal stress is then defined as [11]

$$\sigma_n \times (r,\tau) = \frac{\sigma_n(r,\tau) \cdot (1-v)}{\alpha E (T_\infty - T_0)}, \tag{10}$$

where the subscripts, $n = r$, θ and φ stand for the three directions of the actual stresses in the sphere, respectively.

From Equations (5) and (8)–(10), the dimensionless thermal stress fields that occur in the sphere during the rapid heating or cooling of the surface are readily calculated, as shown in Figure 3(a) and (b). The results indicate that the thermal stresses generated on the surface are tensile during cooling, whereas the thermal stresses presented at the centre are tensile during heating.

In addition, under the condition of the same absolute value of temperature difference, $|T_0 - T_\infty|$, the surface tensile stresses during cooling are much greater than the central tensile stresses during heating. Generally, ceramics are much weaker in tension than in compression, this failure often occurs on the surface during cooling. Accordingly, in the following, we only focus on the tangential tensile thermal stresses on the surface. Let $r = R$, substituting Equations (5) and (9) into Equation (10) gives the tangential stress on the surface

$$\sigma_\theta^*(R,\tau) = \sum_{n=1}^{\infty} A_n \cdot \left(\frac{\sin\beta_n}{\beta_n} + \frac{3\cos\beta_n}{\beta_n^2} - \frac{3\sin\beta_n}{\beta_n^3} \right) \cdot \exp\left(-\beta_n^2 \cdot \frac{a\tau}{R^2} \right), \tag{11}$$

where both β_n and A_n involve Biot number of the sphere, and so naturally, they are associated with the radius of the sphere R. Obviously, in terms of the ceramic spheres with both the same material and service condition, Biot numbers of the spheres are completely determined by their radius. Thus, Equation (11) indicates the evolutions of the thermal stresses that occur on the surfaces of the spheres with different radii during thermal shock, as shown in Figure 4, and the data of h and k are from Table 1 in the

Downloaded by [Institute of Mechanics] at 00:03 02 September 2014

Downloaded by [Institute of Mechanics] at 00:03 02 September 2014

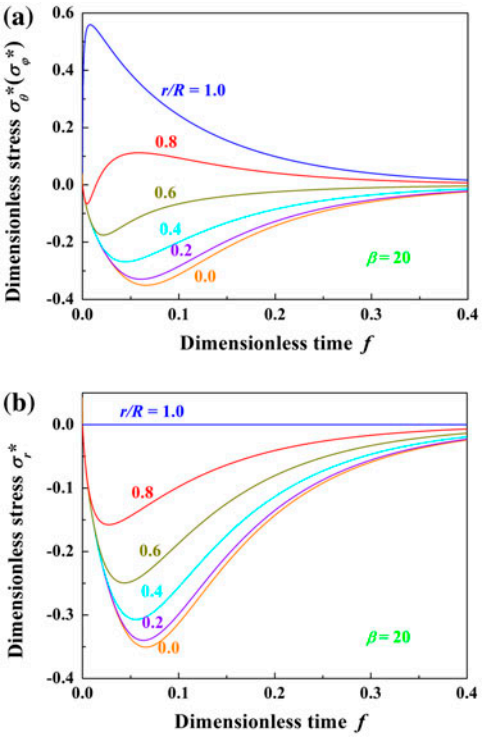

Figure 3. (colour online) The evolutions of the stress fields in the sphere during rapid cooling, (a) the tangential stresses and (b) the radial stress, where the Biot number was taken as $\beta = 20$.

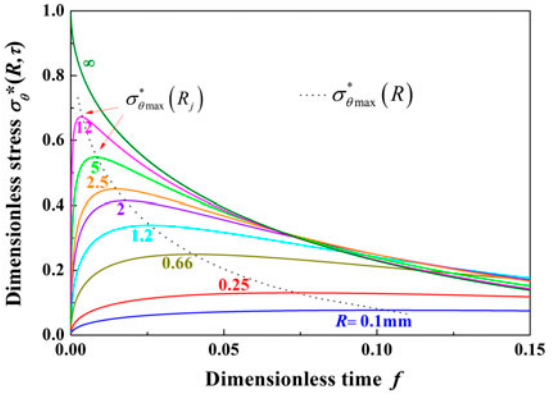

Figure 4. (colour online) The dimensionless stress at the surface of the sphere during thermal shock with different radii R, where the magnitude of $\sigma^*_{\theta\max}(R_j)$ increases with R.

temperature range 20–600 °C. Note that in order to make calculation consistent with the real situation, the properties of alumina are considered to be temperature dependent and average parameters in temperature range are used as a compromise approach. In

Table 1. The average mechanical and thermal parameters of alumina used in calculation.

Temperature range (°C)	Young modulus E (GPa) [12]	Poisson's ratio v	Strength σ_0 (MPa) [12]	Convective heat transfer coefficient h ($W\,m^{-2}\,K^{-1}$)	Thermal conductivity k ($W\,m^{-1}\,K^{-1}$) [13]	Coefficient of thermal expansion α ($10^{-6}\,K^{-1}$) [14]
20–300	383	0.22	386	80,000	24.9	7.0
20–400	382	0.22	374	80,000	22.2	7.3
20–600	380	0.22	358	80,000	18.4	7.7
20–800	378	0.22	347	80,000	15.7	8.0
20–1300	348	0.22	324	80,000	12.0	8.7

Downloaded by [Institute of Mechanics] at 00:03 02 September 2014

addition, the available data of h are dispersed, ranging from 10^4 to $10^5\,W\,m^{-2}\,K^{-1}$ [15–17]. In this paper, we use a more stringent condition, in which h is roughly regarded as a constant and has a value of $80{,}000\,W\,m^{-2}\,K^{-1}$.

Each of the curves in Figure 4 has a maximum value, which is readily determined according to Equation (11). Let $\partial\sigma^*_\theta/\partial\tau = 0$, we obtain

$$\sum_{n=1}^{\infty} A_n \cdot \left(\frac{\sin\beta_n}{\beta_n} + \frac{3\cos\beta_n}{\beta_n^2} - \frac{3\sin\beta_n}{\beta_n^3}\right) \cdot \left(-\beta_n^2 \cdot \frac{a}{R^2}\right) \cdot \exp\left(-\beta_n^2 \cdot \frac{a\tau}{R^2}\right) = 0. \tag{12}$$

Equation (12) stands for the implicit relation between an arbitrary radius R and the time τ. Therefore from Equation (12), we can determine a relation, $\tau = \tau\,(R)$, namely, the time that the thermal stress occurred on the surface of the sphere of radius R reaches its maximum value. Substituting Equation (12), i.e. $\tau = \tau\,(R)$, into Equation (11) gives the form of the maximum stress,

$$\sigma^*_{\theta\max}(R) = \sum_{n=1}^{\infty} A_n \cdot \left(\frac{\sin\beta_n}{\beta_n} + \frac{3\cos\beta_n}{\beta_n^2} - \frac{3\sin\beta_n}{\beta_n^3}\right) \cdot \exp\left[-\beta_n^2 \cdot \frac{a \cdot \tau(R)}{R^2}\right], \tag{13}$$

as shown in Figure 4.

Combining Equation (13) with Equation (10), we obtain the actual maximum thermal stress on the surface of the sphere

$$\sigma_{\theta\max}(\Delta T, R) = \frac{\alpha E \cdot \Delta T}{1-v} \sum_{n=1}^{\infty} A_n \cdot \left(\frac{\sin\beta_n}{\beta_n} + \frac{3\cos\beta_n}{\beta_n^2} - \frac{3\sin\beta_n}{\beta_n^3}\right) \cdot \exp\left[-\beta_n^2 \cdot \frac{a \cdot \tau(R)}{R^2}\right], \tag{14}$$

where $\Delta T = T_\infty - T_0$. This is an indication that the maximum surface thermal stress of the sphere is linearly proportional to the temperature difference and nonlinearly associated with the characteristic dimension of the sphere, as shown in Figure 5(a). In particular, under the condition of the same temperature difference, the larger the characteristic dimension, the greater the maximum surface thermal stress of the sphere; while under the condition of the same characteristic dimension, the higher the temperature difference, the greater the maximum stress, as shown in Figure 5(b) and (c). Here, we employ the average data of alumina in the temperature range 20–600 °C as given in Table 1.

Downloaded by [Institute of Mechanics] at 00:03 02 September 2014

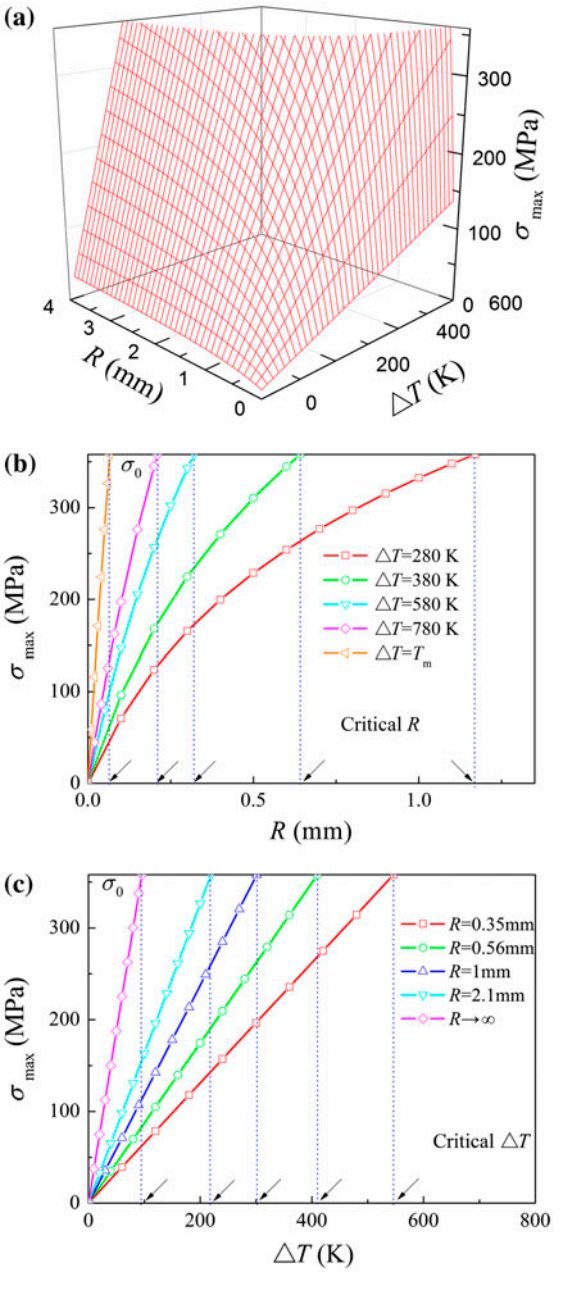

Figure 5. (colour online) (a) The maximum surface stress as a function of R and ΔT; the projection of the maximum surface stress on the plane perpendicular to the axis (b) ΔT and (c) R, respectively, where σ_0 is the inherent strength of the material.

Downloaded by [Institute of Mechanics] at 00:03 02 September 2014

Further, when the maximum surface thermal stresses during heat transfer are greater than the inherent strength of the material of a sphere, the cracks will occur on the surface of the sphere. Thus, according to Equation (14), we obtain the critical curve

$$\sigma_{\theta\max}(\Delta T_c, R_c) = \sigma_0, \tag{15}$$

where σ_0, ΔT_c and R_c are the inherent strength of material, the critical temperature difference and the characteristic dimensional limit, respectively. This critical curve separates the region of $\Delta T - R$ into two parts whether the cracks occur on the surface or not, as shown in Figure 6. This is an indication that as long as the states (ΔT, R) locate under the critical curve, the thermal shock failure of the materials never occurs; no matter how large the characteristic dimension R is and no matter how high the temperature difference ΔT is. Even if an alumina sphere is heated to approach its melting temperature, $T_m = 2054$ °C, the cracks do not occur as long as the radius of the sphere $R < 66$ μm, as shown in Figure 5(b). Likewise, as long as $\Delta T < 96$ K, the cracks never occur no matter how large the radius of the sphere is, as shown in Figure 5(c). For comparison, we also calculate the critical curves using average parameters in different temperature ranges, as shown in Figure 6. We can clearly see that the critical curve gradually moves down with the increase in temperature range.

To verify the results obtained from Equation (15), we compare the experimental data with the theoretical results and find that they have the same tendency. However, for the theoretical results which separate the regions of the crack and the uncracked, only the results using parameters of temperature ranges of 20–400 °C and 20–600 °C are consistent with the experimental results, as shown in Figure 6. This can be ascribed to the fact that the surface heat transfer coefficient largely depends not only on the initial quenching temperature, but also on their evolution in quenching media [18], which affect the theoretical results. In addition, it is generally recognized that alumina has obvious plastic deformation at temperatures higher than 1300 °C and that ceramic specimen of small volume has high strength in statistic [19,20]. According to the critical curve that employs the data in the temperature range 20–600 °C, as shown in Figure 6,

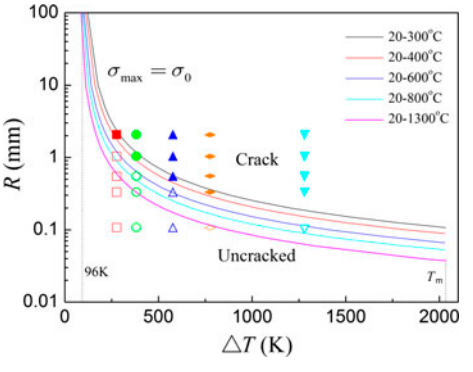

Figure 6. (colour online) The critical curves using parameters of different temperature ranges separate the regions of the crack and the uncracked, and the marks around the curve stand for the experimental data corresponding to Figure 1. The solid marks represent the crack and the hollow marks represent the uncracked regions.

it can be easily derived that in the case of melting temperature, the cracks do not occur as long as the radius of the sphere $R < 66$ μm.

4. Conclusions

Based on the theories of heat transfer and thermal stresses, the characteristic dimensional limit of ceramics together with the critical temperature difference in thermal shock failure is analytically presented. The relation indicates that ceramics become insensitive to thermal shock as soon as the material size becomes smaller than the dimensional limit, or the temperature difference is lower than the critical one. By taking alumina as an illustration, we experimentally demonstrate the relation.

Downloaded by [Institute of Mechanics] at 00:03 02 September 2014

Funding

This work is supported by the National Natural Science Foundation of China [grant number 11102208], [grant number 11232013], [grant number 11021262], and [grant number 11023001].

References

[1] R. Danzer, T. Lube, P. Supancic and R. Damani, Adv. Eng. Mater. 10 (2008) p.275.
[2] W.D. Kingery, J. Am. Ceram. Soc. 38 (1955) p.3.
[3] S.S. Manson, NACA TN 2933 (1953) p.319.
[4] D.P.H. Hasselman, J. Am. Ceram. Soc. 53 (1970) p.490.
[5] Q.N. Liu, F. Song, S.H. Meng and C.P. Jiang, Philos. Mag. 90 (2010) p.1725.
[6] P.F. Becher and W. Warwick, *Factors influencing the thermal shock behavior of ceramics*, in *Thermal Shock and Thermal Fatigue Behavior of Advanced Ceramics*, G.A. Schneider and G. Petzow, eds., Kluwer Academic Publishers, The Netherlands, 1993, p.37.
[7] D. Carolan, A. Ivanković and N. Murphy, J. Eur. Ceram. Soc. 32 (2012) p.2581.
[8] T.J. Lu and N. Fleck, Acta Mater. 46 (1998) p.4755.
[9] P.J. Schneider, *Transient systems, heating and cooling*, in *Conduction Heat Transfer*, Addison-Wesley Publishing, Reading, MA, 1955, p.255.
[10] B.A. Boley and J.H. Weiner, *Some basic problems in thermoelasticity*, in *Theory of Thermal Stresses*, Wiley, New York, 1960, p.302.
[11] W.D. Kingery, H.K. Bowen and D.R. Uhlmann, *Thermal and compositional stresses*, in *Introduction to Ceramics*, Wiley, New York, 1976, p.821.
[12] R. Spriggs, J. Mitchell and T. Vasilos, J. Am. Ceram. Soc. 47 (1964) p.325.
[13] T.L. Bergman, A.S. Lavine, F.P. Incropera and D.P. Dewitt, *Fundamentals of Heat and Mass Transfer*, Wiley, Hoboken, 2011, p.987.
[14] D.L. Jiang, L.T. Li, S.X. Ouyang and J.L. Shi, *China Materials Engineering Canon*, Chemical Industry Press, Beijing, 2006, p.35.
[15] J.P. Singh, Y. Tree and D.P.H. Hasselman, J. Mater. Sci. 16 (1981) p.2114.
[16] P.F. Becher, J. Am. Ceram. Soc. 64 (1981) p.C17.
[17] Y. Kim, W.J. Lee and E.D. Case, Mater. Sci. Eng. A 145 (1991) p.L9.
[18] Z.L. Zhou, F. Song, Y.F. Shao, S.H. Meng, C.P. Jiang and J. Li, J. Eur. Ceram. Soc. 32 (2012) p.3033.
[19] W. Kollenberg, J. Mater. Sci. 23 (1988) p.3321.
[20] Z. Bažant, Arch. Appl. Mech. 69 (1999) p.704.